Event-Related Potentials and Fast Optical Imaging of Cortical Activity During an Auditory Oddball Task

Manon E. Jaquerod, Ramisha Knight, Alessandro E. P. Villa, and Alessandra Lintas

Abstract Event-related potentials (ERP) have been repeatedly used to study the spatiotemporal dynamics of the attentional response in the well-known oddball paradigm. We combined electroencephalography (EEG) with frequency-domain near-infrared spectroscopy (fNIRS) of the frontal cortex to measure neuronal activity with a high spatial and temporal resolution. The aim of this study was to determine the precise chronology of event-related optical signals (EROS) and their consistency with ERPs. In agreement with previous studies, the oddball condition produced larger waveforms for rare (1500 Hz pure tone) with respect to frequent stimuli (1000 Hz), with N1, P2, N2, P3a, and P3b components. At a latency corresponding to the mismatch negativity/N2 wave component, EROS showed the organization of a complex activity in a functional network of frontal areas, with rare tones activating the left premotor dorsal cortex and the left inferior frontal cortex and decreasing the activity of the right superior frontal gyrus. Rare tones elicited also a strong N500 (N400-like) wave component that EROS contributed to localize at the level of the right medial frontal gyrus by EROS. The simultaneous recording of fNIRS and EEG measure-

---

M. E. Jaquerod (✉) · A. E. P. Villa · A. Lintas
NeuroHeuristic Research Group, University of Lausanne, Internef 138, Quartier UNIL-Chamberonne, 1015 Lausanne, Switzerland
e-mail: manon.jaquerod@unil.ch
URL: http://www.neuroheuristic.org

A. E. P. Villa
e-mail: alessandro.villa@unil.ch

A. Lintas
e-mail: alessandra.lintas@unil.ch

A. E. P. Villa
LABEX, HEC Lausanne, Faculty of Law, Criminal Justice and Public Administration, University of Lausanne, Quartier UNIL-Chamberonne, 1015 Lausanne, Switzerland

R. Knight
University of Illinois, 2111 Beckman Institute, 405 North Mathews Avenue,
Urbana, IL 61801, USA
e-mail: rsknight@illinois.edu

A. Lintas et al. (eds.), *Advances in Cognitive Neurodynamics (VII)*, Advances in Cognitive Neurodynamics,
https://doi.org/10.1007/978-981-16-0317-4_18

ments with high temporal accuracy over the human prefrontal cortex supports the potential for this approach to unravel the functional cortical network involved in cognitive processing.

1 Introduction

A fundamental property of animal behavior is habituation, i.e., the decrement of response with repeated stimulation, which is a necessary process to detect deviant or novel stimuli (Blumstein, 2016; Thompson, 2009). A classical paradigm, called "oddball" paradigm, used to study the responsiveness to a repeated auditory stimulus consists of a long sequence of repetitive identical stimuli (the frequent stimuli) that is replaced with a low probability, and at random, by a different stimulus (the rare stimulus). Brain activity elicited by frequent and rare stimuli has been recorded by electrophysiological means to study the brain processes underlying attention switches to, and involuntary discrimination of, rare among the frequent stimuli. Animal studies showed that responses at the level of the cerebral cortex are associated with attentional circuits that are strongly affected during anesthesia (Apelbaum et al., 1960; Eriksson & Villa, 2005; Ruusuvirta et al., 1996).

In humans, the oddball paradigm was implemented in active and passive conditions (Näätänen, 1990; Squires et al., 1975). The active condition is an attentional task, such that the participant must attend to all stimuli in order to detect the rare stimuli and generate a motor response, e.g., a key-press. In the passive condition, the participant is usually instructed to ignore all stimuli and to attend other stimuli, usually presented in another sensory modality. Maintaining a goal-directed behavior that requires selective attention, brain responses to the habituation of the frequent stimuli, and the salient perception of rare stimuli may bring insights about reorientation of attention. The oddball paradigm has been extensively studied by electroencephalography (EEG), i.e., by measuring variations in the electric field at the scalp induced by the summation of mass neuronal firing rates with a millisecond-level of resolution. The selective sensitivity of the technique for brain layers with correlated dipoles makes neural activity in sulci far less represented in the EEG signal than neural activity in gyri (Nunez, 1995). Furthermore, the spatial filtering of fields by the head volume conductor implies interdependencies of measurements between electrode sites and strongly restrain the capacity for EEG to depict the precise spatial distribution of patterns of activity (Nunez, 1995). The event-related potentials (ERPs) are obtained by averaging, over many trials, the EEG signal variations triggered by sensory or behavioral events. Endogenous ERPs are thought to reflect the neurophysiological correlates of cognitive processes.

In the oddball paradigm, the auditory stimuli elicited ERPs characterized by several components (N1, P2, N2, P3) whose latencies and amplitudes differentiated rare from frequent stimuli (Alexander et al., 1994; Michalewski et al., 1986; Näätänen, 1990). The N1 wave is generated by a stimulus-driven attention-trigger mechanism (Näätänen & Picton, 1987). A positive component P2 of the ERP is often preceding the negative component N2 at approximately 250 ms after rare stimuli (Goodin et al., 1978). This wave may often be dissociated into an earlier fronto-central N2a component (also known as "mismatch negativity") and a later, more frontally distributed, N2b component associated with the allocation of attention to the eliciting stimulus in the active oddball condition (Näätänen, 1990; Squires et al., 1975). The mismatch negativity (MMN), characterized by its responsiveness to low probability stimuli even in the passive auditory oddball condition, may underlie the ability to discriminate acoustic differences, a fundamental aspect of sensory perception. The N2 is followed by the P3 (P300) component, with larger amplitude in active than in passive conditions, formed by a fronto-central wave complex N2-P3a that can be dissociated from a temporo-parietal P3b wave (Molnár, 1994; Näätänen, 1990; Polich, 2007; Squires et al., 1975; Verleger, 1988). In addition, at 400–500 ms from stimulus onset, the rare stimuli elicited a slow frontally maximal negativity, referred to as N500 (N400-like) (Gaillard, 1976).

Signals recorded by functional magnetic resonance imaging (fMRI) are associated with the blood-oxygen-level-dependent (BOLD) signal, an hemodynamic indirect measure of neural activity with severe limitations in temporal resolution and with challenging interpretation to make deductions about the nervous system. The activation of spatially limited neuronal populations may not be strong enough to produce significant hemodynamic changes, but still produce a significant ERP wave. Brain imaging with fMRI has been used to localize the brain areas activated during the P3 wave elicited by the oddball paradigm (Linden et al., 1999; McCarthy et al., 1997; Menon et al., 1997). In fMRI studies, the detection of rare stimuli in oddball tasks related to BOLD signal increased in the supramarginal (Horovitz et al., 2002; Mangalathu-Arumana et al., 2012; McCarthy et al., 1997; Menon et al., 1997) and superior temporal gyri (Mangalathu-Arumana et al., 2012; Opitz et al., 1999), in agreement with greater wave amplitude of P3b observed at the temporal/parietal electrode sites of EEG. A significant hemodynamic response was also reported in the frontal lobe, in particular at the level of the middle frontal gyrus (MFG) (Horovitz et al., 2002; McCarthy et al., 1997; Stevens et al., 2005), frontal midline areas (Menon et al., 1997) an the opercular area of the inferior frontal gyrus (IFG), corresponding to Brodmann area 44 (Linden et al., 1999). The ERP response to the oddball paradigm is complex and cannot be reduced to its P3 component. Besides the spatial dependency of its signal on the location of blood vessels, fMRI relies on an indirect correlate of neural activity which is intrinsically too slow to reveal the complexity of neurodynamics. Hence, it is likely that BOLD fMRI signal generation reflects the sustained activity of a large neuronal system triggered by the rare stimuli and that brief synaptic activity, evoked by those stimuli in dynamic neural circuits, might be detectable only with methods characterized by signal-to-response dynamics faster than neurovascular signals.

Transcranial near infrared spectroscopy (NIRS) allows the non invasive differentiation between tissues with different light attenuation or scattering properties and can provide spectroscopic information on the concentrations of chromophores, in particular oxy- and deoxy-haemoglobin, HbO2 and Hb (Chance et al., 1993; Delpy & Cope, 1997; Gratton et al., 1995; Scholkmann et al., 2014; Strait & Scheutz, 2014;

Torricelli et al., 2014). A slow hemodynamic signal, corresponding to cerebral blood oxygenation variations, is measured as a function of near-infrared light propagation through extra-cerebral and cerebral tissue. Both the optical path length and the cerebrospinal fluid layer affect the measurement, but the geometry of the sulci and the boundary between the gray and the white matter have little effect on the detected light distribution (Okada et al., 1997). The NIRS hemodynamic signal, which is similar to the BOLD signal measured by fMRI, is modified by neuronal activity through neurovascular coupling with latencies of several seconds. In addition to the measurement of changes in light intensity, fNIRS instruments with a frequency-domain technology of measurement allow the recording of a fast optical signal with a latency in the order of milliseconds (Gratton & Fabiani, 2010). This measurement, made possible by the modulation of light sources at a high radio-frequency (e.g., 110 MHz), is based on a complex function of the tissue absorption and scattering coefficients to include changes in light intensity with distance, phase, and modulation depth changes of intensity-modulated light and the temporal dispersion of light from an ultrashort input light pulse (Gratton et al., 1997; Gratton & Fabiani, 2001; Wolf et al., 2002). Neural activity can be directly detected by fast fNIRS signal through changes in the scattering coefficient of the brain tissue. A change in neuronal cell volume following an action potential discharge is meant to account for subtle, yet measurable, variation in the scattering properties of the tissue (Lee & Kim, 2010; Steinbrink et al., 2000; Villringer & Chance, 1997). Although optical imaging with fast fNIRS signals has the potential for a millimeter-level of spatial resolution, it is limited to brain regions located only few centimeters below the scalp (Gratton et al., 1997).

The two main cortical associative auditory pathways include a posterior dorsal stream processing spatial (“where”) information from the posterior superior temporal gyrus (STG) to the parietal cortex, and an anterior ventral stream processing an object (“what”) from the anterior part of STG to IFG (Ahveninen et al., 2006). Both pathways send projections to the prefrontal cortex with dorsal (DLPFC) and ventral (VLPFC) regions involved in different roles during the processing of auditory information with high cognitive load (Plakke & Romanski, 2016). Simultaneous recording of ERP and the corresponding NIRS response has recently raised considerable interest to complement the study of the spatial distribution of cortical and subcortical activation during oddball and go-nogo tasks. Source localization based on the NIRS slower hemoglobin response showed significant oddball activation in temporal/parietal areas (Kennan et al., 2002) with a gender effect suggesting females’ event-categorization process is more efficient than in males (Jausovec and Jausovec, 2009), and activation of MFG by tasks that require heavy cognitive processing (Jeong et al., 2018). Stronger hemodynamic responses were reported in the left prefrontal cortex when participants were performing an auditory oddball task under mental stress (Liu et al., 2011), but the response was stronger in the right VLPFC when attending to stimuli that required higher cognitive load and negatively correlated with the level of state anxiety (Tseng et al., 2018). The averaging of optical responses evoked by the repetition of the same stimulus allowed the analysis of event-related transient optical responses based on continuous wave measurements of light intensity (Kubota et al., 2008; Medvedev et al., 2008) and the development of event-related optical signal (EROS) analysis by means of frequency-domain instruments, based on a measurement of phase-shifts of the fast optical signal as the photons migrate through the brain tissue, which is optically modified by neural activation (Gratton & Fabiani, 1998). In passive detection of deviant auditory stimuli, source localization by EROS reported early activity co-occurring with ERP waves localized in the auditory areas of STG (Rinne et al., 1999) followed by activation of VLPFC in pre-attentive auditory change detection (Tse et al., 2013). At a later latency, consistent with P3 and frontal negativity, EROS data have shown activation in the right MFG (DLPFC) by rare stimuli during an auditory oddball task (Low et al., 2006).

In this study, we analyzed ERPs and EROS in the frontal cortex elicited by a passive two-tone auditory oddball discrimination task. The task consisted of a random stream of frequent auditory tones (1000 Hz, $p = 92\%$) or an infrequent oddball auditory tone (1500 Hz, $p = 8\%$) being played at a constant interval of 1600 ms. In this paradigm, attention is directed away from the acoustic stimuli with an explicit instruction to fixate on a white cross centered on a screen. Our EROS analysis was mainly based on changes in the phase delay because it has the advantage of a greater sensitivity for deeper locations and a greater spatial resolution than light intensity measurements (Gratton & Fabiani, 2010). These results indicate that the passive auditory oddball task modulated the brain activity measured by EROS in the frontal cortex within the same time range as EEG measures. The simultaneous recording of fNIRS and EEG measurements with high temporal accuracy over the human prefrontal cortex supports the potential for this approach to unravel the functional network involved in cognitive processing.

2 Methods

2.1 Participants

Ten healthy volunteers participated in the study (mean age = 28.1 years; 6 women). All subjects were right-handed and reported normal hearing and normal or corrected-to-normal vision. Prior to participation, subjects were informed about the procedure and provided signed informed consent for their participation in line with the Declaration of Helsinki (World Medical Association, 2013) and the recommendations of ethical and data security guidelines of the University of Lausanne. Two subjects (1 male and 1 female) were treated as pilot data and were excluded from the analysis.

2.2 Procedure

The task consisted of 12 blocks with 120 trials each, following the passive auditory oddball paradigm. Frequent (1000 Hz at occurrence probability $p = 92\%$) and a rare (1500 Hz, $p = 8\%$) computer generated tones, lasting 500 ms, were presented at approximately 60 dB SPL. Each block consisted of a randomized sequence of frequent and rare tones where stimuli onsets were separated by 1600 ms. Subjects were only instructed to watch a white fixation cross in the center of a computer screen placed horizontally at 65 cm in front of the middle of their eyes. In order to minimize the noise added by environmental light in the NIRS data, experiments were run with the lights off and the computer screen background was black.

2.3 Electrophysiological Recording

Continuous EEG was recorded using 64 scalp Ag/AgCl active electrodes (ActiveTwo MARK II Biosemi EEG System, BioSemi B.V., Amsterdam, The Netherlands), sampled 1024 Hz and referenced to the linked mastoids. Impedance was kept below 20 kΩ. Electrodes were mounted on a head-cap (10/20 layout, NeuroSpec Quick Cap) that was modified in order to allow the optical equipment to have direct contact with the scalp (Fig. 1a). Data were preprocessed and analyzed with the EEGLAB toolbox (MATLAB, The MathWorks, Inc.) (Delorme & Makeig, 2004). EEG data were then segmented into epochs using markers. Epochs of the continued data with visible large movement artifacts were removed from the analysis. A poor EEG signal from a selected electrode was reconstructed by combining signals from neighbor-

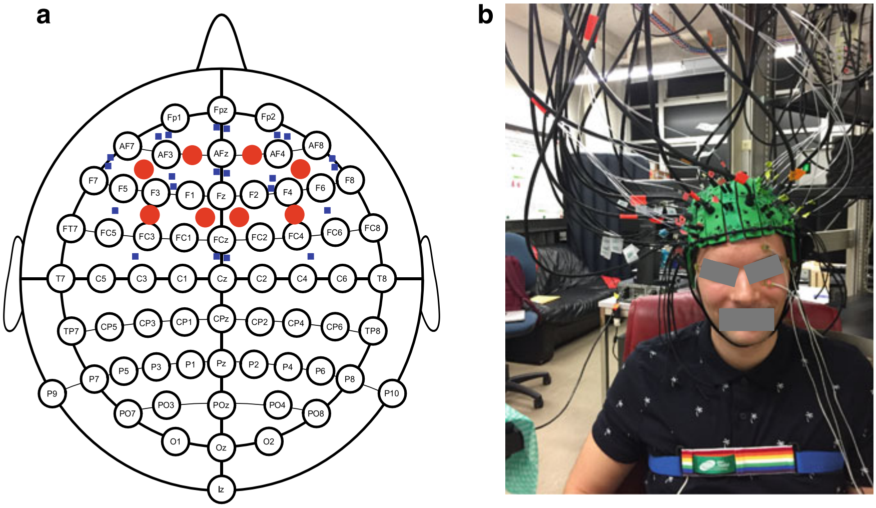

Fig. 1 **a** Schematic representation of the co-localization of the 8 light detectors (red circles) and 22 light sources (blue squares) over prefrontal and premotor areas of the cerebral cortex and the 64-channel electrophysiological setup with the standardized International 10/20 system. **b** The photo-multiplier tube detectors and fiber optic bundles placed over the participant's forehead using a custom-made mounting system

ing electrodes using interpolation. The EEG signal was decomposed using an Infomax Independent Component Analysis (ICA) in order to correct eye blink artifacts. Epochs containing visible artifacts after ICA preprocessing were rejected. All epochs kept for the analysis were bandpass filtered between 0.1 and 40 Hz before ERPs were computed.

A grand average of the ERP response to the oddball task was calculated by averaging individual participants' ERPs. In this study, we report data recorded at electrode sites Fz, Cz, and Pz, separately for frequent and rare tones. The amplitude was calculated as the voltage difference between a pre-stimulus baseline and the respective peak. The latency was defined by the lag for the ERP wave to reach its peak amplitude. We focused our topographic analysis on the time windows corresponding to the main ERP components. The N1/P2 was identified as negative deflection between 120 and 150 ms post-stimulus followed by a positive deflection between 170 and 230 ms post-stimulus. The MMN/N2 was identified as the largest peak occurring 230–260 ms after stimulus presentation, the P3a as the positive deflection between 280 and 300 ms and the P3b as the largest peak occurring 350–400 ms after stimulus presentation. A large negative wave between 460 and 650 ms post-stimulus characterized the N500 (N400-like) component of the ERP.

2.4 Optical Recording

Optical data were collected using a frequency-domain NIRS system ISS Imagent (Champaign, Illinois, USA) with 8 detectors and 22 frequency-modulated light (830 nm wavelength modulated at 110 MHz) sources. The sources and detectors were co-located with the EEG setup, as shown in Fig. 1a. In the present study, EROS was recorded with source-to-detector distances between 20 and 55 mm. The fiber optic bundles connected to the laser diodes emitting light sources and the fiber optic bundles connected to the detectors (photomultiplier tubes) were held in place using a custom-built head mounting system (Fig. 1b). Detectors amplifiers' were modulated at a frequency of 110.005 MHz. Hence, a heterodyning frequency (or cross-correlation frequency) was generated equal to the difference between the frequency modulation of the sources and detectors, i.e. 5000 Hz, thus implying a period of oscillation of 0.2 ms. The photomultiplier output current was Fast Fourier Transformed (FFT) on four oscillations (i.e., 0.8 ms). One oscillation was skipped in order to avoid cross-talk between sources, thereby yielding a data acquisition period of 1 ms for each source. Light sources were time multiplexed in a cycle of eight per sampling point, which corresponds to an effective time resolution of 8 ms (i.e., an effective sampling rate 125 Hz). Notice that for each data point, we measured the DC (average) intensity, AC (amplitude) intensity, and relative phase delay.

The locations of each source and detector were digitized with a 3D digitizer (FASTRAK 3Space, Polhemus Inc.). Phase delay measurements in the cross-correlation signal were corrected off-line for phase wrapping and their mean was adjusted to zero. The algorithm described in Gratton and Corballis (1995) was used to remove the pulse artifacts from the signal. Only channels with phase standard deviation smaller than 200 ps were included for further analysis (Gratton et al., 2006). Data were bandpass filtered between 0.1 and 10 Hz before statistical topographical surface projection maps of fast optical signals were computed using the Opt3D software (Gratton, 2000) available at the NeuroImaging Tools & Resources Collaboratory (https://www.nitrc.org/). EROS data were spatially filtered with an 8-mm Gaussian kernel and for each subject, contrast, and voxels, t-scores were computed and converted to Z-scores. This approach removes emphasis on larger effects in relation to the smaller effects and was chosen because of our small sample size ($N = 8$).

The regions of interests (ROIs, cf. Table 1 and Fig. 2) were selected on the basis of previous studies on auditory deviance detection. The Talairach space boundaries of our ROIs were kept consistent with anatomical structures and we assigned each ROI to a Brodmann area with the BioImage Suite software package (http://www.bioimagesuite.org, Lacadie et al., 2008).

Table 1 Coordinates (x, y, z) are in Talairach space (Talairach & Tournoux, 1988) of the areas studied here

Region	Left	Right	Broadmann area
Superior frontal gyrus (SFG)	$x \in [-35, -15]$	$x \in [30, 10]$	BA 9/BA 8
	$y \in [25, 55]$	$y \in [25, 55]$	
	$z \in [50, 35]$	$z \in [50, 35]$	
Middle frontal gyrus (MFG) dorsolateral prefrontal cortex (DLPFC)	$x \in [-50, -35]$	$x \in [45, 30]$	BA 46 (/BA 10), BA 8 / BA 9
	$y \in [25, 55]$	$y \in [25, 55]$	
	$z \in [30, 15]$	$z \in [20, 30]$	
Inferior frontal gyrus (IFG) ventrolateral prefrontal cortex (VLPFC)	$x \in [-60, -45]$	$x \in [60, 45]$	BA 44 (/BA 45)
	$y \in [15, 30]$	$y \in [15, 30]$	
	$z \in [15, 30]$	$z \in [15, 30]$	
Dorsal premotor (PMd) cortex	$x \in [-40, -15]$	$x \in [35, 10]$	BA 6
	$y \in [25, 55]$	$y \in [25, 55]$	
	$z \in [45, 60]$	$z \in [45, 60]$	

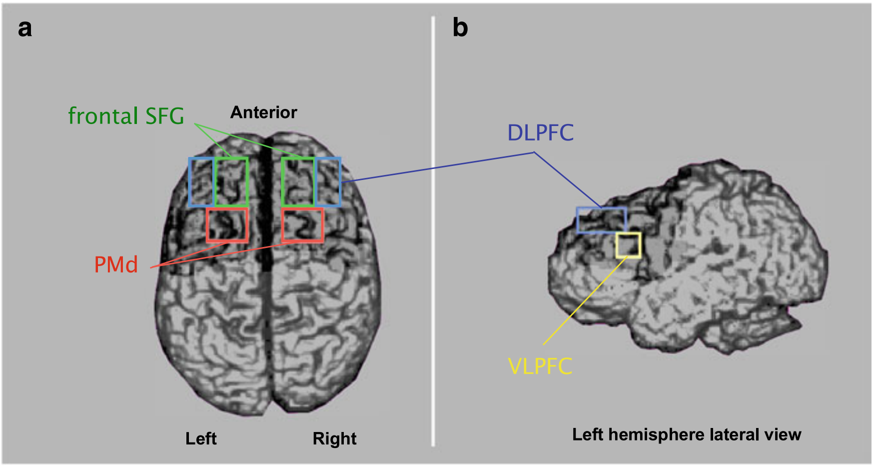

Fig. 2 Antero-posterior (**a**) and left hemisphere lateral (**b**) views of selected regions of interest (ROIs). The area in darker grey represents the brain region sampled by the recording montage. VLPFC: ventrolateral prefrontal cortex; DLPFC: dorsolateral prefrontal cortex; SFG: superior frontal gyrus; PMd: dorsal premotor cortex

3 Results

3.1 Grand Average ERPs

The sample size for the ERP analysis was $N = 7$ because one more subject (male) was excluded due to a technical problem that occurred during EEG data collection. The frequent and rare tones elicited similar negative ERP component between 120 and 150 ms (N1), followed by a small positive wave P2 (P180), along the midline sites, somewhat larger in the rare condition and towards frontal areas (Fig. 3a, B1). A second ERP peak negativity was mainly elicited in the rare tone condition at 230–260 ms post-stimulus (MMN/N2) at all three midline sites (Fig. 3a). We observed distinct topographic maps of electrical activity between the conditions during this time window (Fig. 3B2), but it was significantly different from the frequent tone ERP only on the frontal site ($p < 0.05$, Bonferroni-corrected for 64 electrodes). It is possible that such fronto-central N2 wave is a composite of N2a and N2b components, which overlap in time and scalp distribution.

Consistently with the literature, a significant difference between the two conditions ($p < 0.05$, Bonferroni-corrected for 64 electrodes) appeared for a large positive deflection elicited with a lag of approximately 300–400 ms (P300) after rare tones at all reported electrode sites. This positive wave included a fronto-central component P3a (Fig. 3B3) peaking between 280 and 330 ms and a second component P3b with

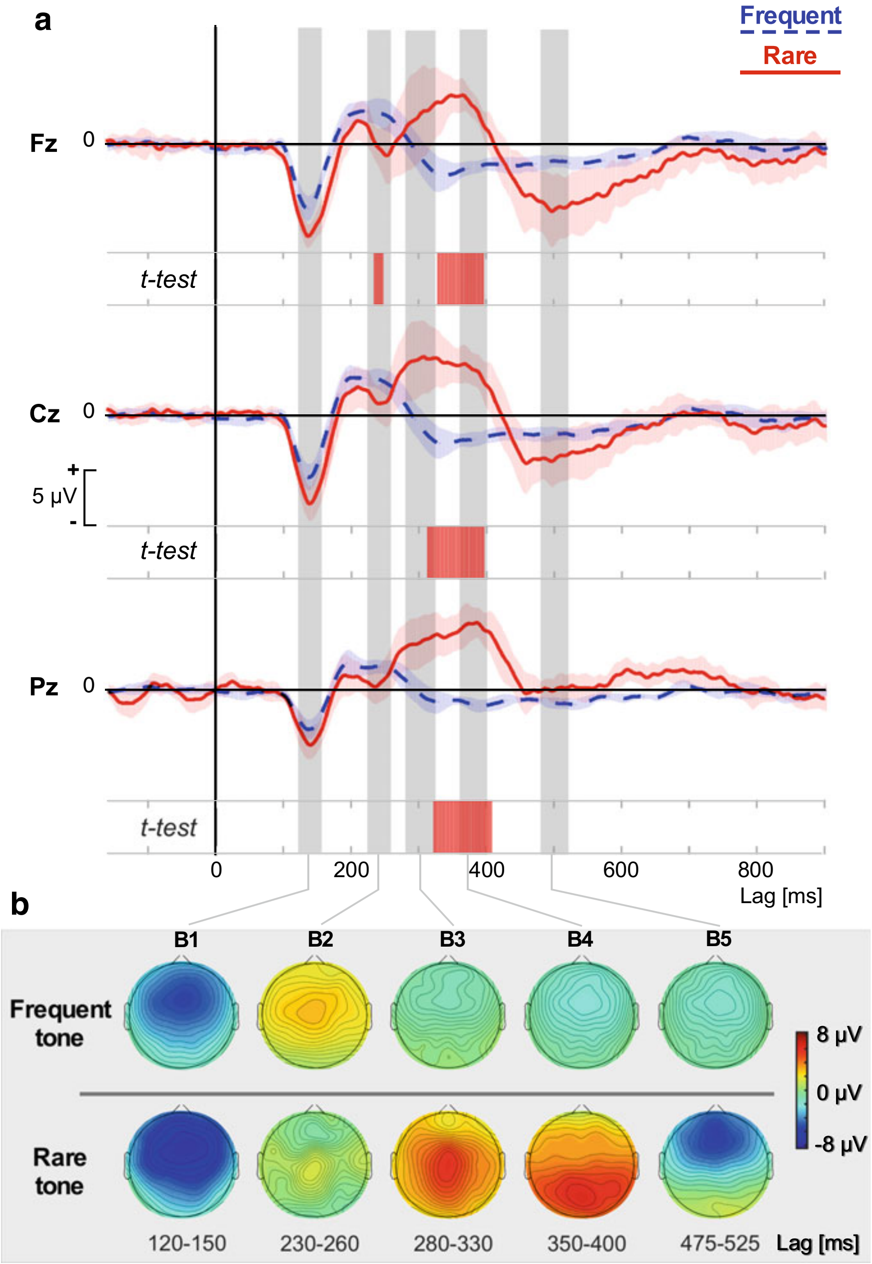

Fig. 3 **a** Grand average ERP waveforms (mean ± 2× SEM) at electrode sites Fz, Cz and Pz ($N = 7$ participants). Each plot is followed by the result of a paired t-test between the frequent (dashed blue) and rare (red) tones (Bonferroni-corrected for 64 electrodes, in red when $p < 0.05$). **b** Topographic maps of scalp potential distribution at the main ERP components. **B1**: N1 at 120–150 ms post-stimulus; **B2**: MMN/N2 at 230–260 ms; **B3**: P3a at 280–330 ms; **B4**: P3b at 350–400 ms; **B5**: N500 (N400-like) at 475–525 ms

a posterior maximum (Fig. 3B4), peaking between 350 and 400 ms. A large frontal negativity observed between 450 and 600 ms (N400-like/N500) was characterized by maximal response over midline frontal electrodes (Fig. 3B5).

3.2 EROS

The data acquisition problem encountered during EEG recording of one participant did not affect fNIRS, therefore the sample size for the EROS analysis was $N = 8$. The spatiotemporal profile of the optical signal response corresponded to the topographical maps on group-level Z statistics of a 'differential EROS response', which resulted from the contrasts conducted within the ROIs for each condition separately relative to pre-stimulus baseline and for rare versus frequent tones, to the three time points of the peak contrasts, i.e. at 40, 256, and 480 ms (Fig. 4).

Rare tones elicited less bilateral activation compared to frequent tones between 32 and 40 ms following the stimulus onset (Fig. 4A). In the left hemisphere, the negative peak voxel activity was located in the Brodmann Area BA46 (DLPFC, ROI in blue in Fig. 2, Talairach coordinates $x = -43$, $y = 27$) and did not reach ($Z = -2.135$) the level of significance ($p = 0.05$) when averaging the voxels within the ROI ($Z_{\text{crit}(0.05)} = -2.60$). The right negative peak voxel activity belonged to the posterior part of BA8 ($x = 24$, $y = 27$) across superior frontal gyrus (ROI in green in Fig. 2) and did not reach the ROI significance criterion ($Z = -2.169 > Z_{\text{crit}(0.05)} = -2.85$).

At 256 ms post-stimulus, Fig. 4b shows the statistical maps resulting from differential EROS responses and Fig. 5 shows also the responses in the rare and frequent tone conditions, representing a complex pattern of activity co-occurring with N2 component of the ERP. Between 240 and 272 ms in the rare tone condition, we observed greater activation ($Z > 2$) in the ROI corresponding to the left PMd (ROI in red in Fig. 2, $x = -21$, $y = 12$, BA6) with a peak voxel activity at 256 ms ($Z = 2.263 < Z_{\text{crit}(0.05)} = 2.67$). Between 240 and 264 ms, we observed a reduced differential EROS response in the right SFG (BA8, $x = 24$, $y = 29$) with a peak voxel activity at 256 ms ($Z = -2.368 > Z_{\text{crit}(0.05)} = -2.89$). Those two effects were very close to their ROI criterion of significance at $p = 0.05$.

Broca's area (VLPFC, ROI in yellow in Fig. 2, $y = 22$, $z = 22$), corresponding to BA44 contained and limited by pars opercularis of the left inferior frontal gyrus, was characterized by a greater activation in the rare tone condition in the interval 248–264 ms with a significant peak voxel activity at 264 ms ($Z = 2.234 > Z_{\text{crit}(0.05)} = 2.20$). This ROI was activated almost exclusively during the rare tone condition, as emphasized by the significant contrast (maximum at 272 ms, $Z = 2.245 > Z_{\text{crit}(0.05)} = 2.19$) of this condition with the baseline between 248 and 280 ms (Fig. 5b, sagittal projection). In the left hemisphere, it is interesting to notice also an activation at the level of the auditory cortex in the postcentral gyrus (BA 43) only after frequent tones (Fig. 5c). This activation fell below a significant contrast ($Z < 2$) and was not visible in the differential EROS response (Fig. 5a).

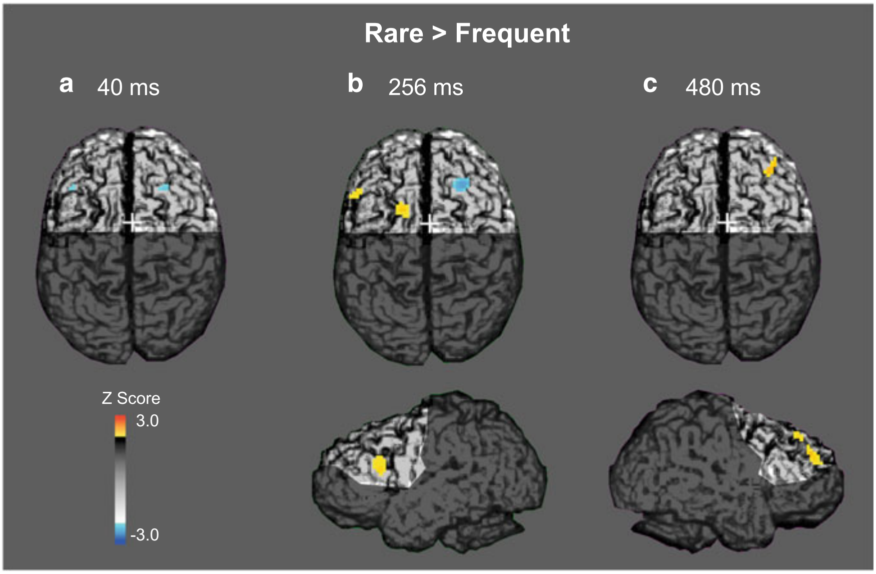

Fig. 4 Spatial maps based on group-level ($N = 8$) Z statistics for the EROS data contrasting rare versus frequent tones in the passive auditory oddball task relative to the pre-stimulus baseline. The area in light grey represents the brain region sampled by the recording montage. **a** Projection of EROS data to the axial surface at 40 ms after stimulus onset. The differential EROS response shows that superior frontal gyrus was activated after frequent tones by the dorsal spatial ("where") processing stream, BA46 in the left hemisphere and BA8 in the right hemisphere. **b** Spatial maps of the EROS data projected to the axial (top) and left sagittal (bottom) surfaces of significant ROIs at 256 ms after stimulus onset, co-occurring with N2b ERP wave. Notice the complex pattern of response, see Fig. 5 for more details. **c** Projection to the axial (top) and right sagittal (bottom) surfaces of significant ROIs at 480 ms after stimulus onset, co-occurring with N500 (N400-like) ERP wave. In the right hemisphere, notice the strong activation of DLPFC after rare tones at the level of BA9 (axial projection) and BA46 (sagittal projection)

In the right middle frontal gyrus (Fig. 4C), at the level of BA9 of DLPFC (Talairach coordinates $x = 32$, $y = 39$), a greater activation was observed between 464 and 520 ms in the rare tone condition with a peak voxel activity at 488 ms ($Z = 2.361 < Z_{\mathrm{crit}(0.05)} = 2.97$). This activation co-occurred with the N500 (N400-like) ERP wave. A more anterior part of DLPFC, corresponding to BA46 (see the right hemisphere sagittal view of Fig. 4c), was also activated by the differential EROS response during this interval, but it was located outside the predefined ROIs.

4 Discussion

We report results on the neural dynamics of frontal cortex response to a passive auditory oddball task studied by simultaneous recording of fast optical signals with high temporal resolution (EROS) and ERPs. To the best of our knowledge, no other

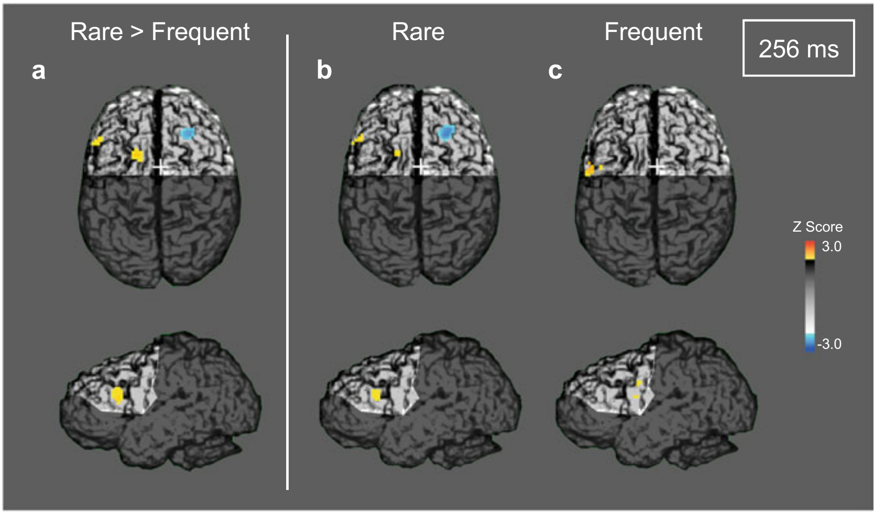

Fig. 5 Spatial maps based on group-level ($N = 8$) Z statistics for the EROS data at 256 ms after tone onset, co-occurring with N2b ERP wave, projected to the axial (top) and left sagittal (bottom) surfaces. **a** Response contrasting rare versus frequent tones compared to pre-stimulus baseline, same as Fig. 4b. **b** Response to rare tones separately contrasted with pre-stimulus baseline. Notice the same ROIs visible in panel (**a**), although with a different significant voxel density. **c** Response to frequent tones contrasted with pre-stimulus baseline. Notice a small activation in the postcentral gyrus, at the border of the area under investigation

study has yet combined EROS with a similar temporal resolution (i.e. 8 ms sampling time) with a 64-channel EEG system in an auditory oddball task. Electrophysiological recordings revealed all the ERP components (N1, P2, N2, P3) well described in the literature (Alexander et al., 1994; Michalewski et al., 1986; Näätänen, 1990). We observed also several commonalities and some differences regarding the brain areas and the response timing with the few previous studies reporting EROS analyses in auditory and visual oddball tasks (Low et al., 2006; Proulx et al., 2018; Tse & Penney, 2008; Tse et al., 2006, 2013). Despite controversial observation about the significance of fast optical signals measured by fNIRS (Steinbrink et al., 2005; Syré et al., 2003), the co-occurrence of optical signals and ERP waves found here confirms that such a methodological approach carries the potential for investigating neurodynamics of cognitive activity in a wide range of tasks (Gratton et al., 2018). However, there are several limitations that should be acknowledged in our results. First, this study may be considered somewhat preliminary because of the small sample size ($N = 7$ for ERP and $N = 8$ for EROS analyses), although the statistical analyses showed suitable effects. Additional data are being collected and a final report with a larger sample will be soon completed. Second, fast optical signals suffer from a low signal-to-noise ratio and the response signal is limited to a few centimeters below the scalp (Gratton & Fabiani, 2010). It is important to underline that complementary studies using different and independent measures of brain activity are necessary to gain further insights of the spatiotemporal patterns of brain dynamics while performing behavioral tasks.

After the stimulus onset, the earliest response observed in this study is an optical signal in the differential EROS response, appeared as early as between 32 and 40 ms post-stimulus showing a bilateral activation that is larger for frequent than rare stimuli, thus suggesting a short latency input from the auditory system. The localization of the signal at the level of BA46 of DLPFC in the left hemisphere and at the level of BA8 of the superior frontal gyrus in the right hemisphere suggests that the input is not from the sensory ascending subcortical pathway. The DLPFC is the end point for the dorsal stream that transmits spatial ("where") information (Ahveninen et al., 2006; Plakke & Romanski, 2016).

The next evoked activity response was an ERP component with a negative peak observed along the midline, mainly fronto-central sites, between 120 and 150 ms post-stimulus followed by a smaller positive wave. The profile and the latency of this wave was similar after frequent and rare tones, although the amplitude after rare tones tended to be larger. The latency and localization of this peak is in agreement with the N1/P2 (N100-P200) complex reported for the auditory oddball task with strong generators in the auditory areas of the STG and with association with a stimulus-driven attention-trigger mechanism (Näätänen & Picton, 1987; Rinne et al., 1999). In previous imaging studies coupled with EEG, the N100 component during auditory tasks co-occurred also with a signal in the anterior cingulate cortex (ACC) (Esposito et al., 2009; Walz et al., 2013). At this latency, we could not observe any significant optical response in our ROIs of the prefrontal cortex. This is likely due to the fact that our fNIRS montage was not designed to record neither from the auditory cortex nor from ACC.

The typical event-related response to the stimulus presentation observed in the auditory oddball task is the N2/P3 (P300) wave complex (Alexander et al., 1994; Fabiani & Friedman, 1995; Näätänen & Picton, 1987; Squires et al., 1975). This wave is characterized by several components, which may overlap in time and scalp distribution. We observed a fronto-central N2b-P3a component (Fig. 3B2 and B3) between 230 and 330 ms post-stimulus, followed by a P3b component with a parietal maximum (Fig. 3B4), peaking between 350 and 400 ms. Source locations determined from fMRI showed that the ACC was the principal generator of N2b-P3a ERP wave following dipole modeling of ERPs (Crottaz-Herbette & Menon, 2006). We observed fast optical signals correlated with the timing of this wave, but their latency was different (up to approximately 100 ms later) than the lag reported from other oddball-related EROS analyses (Low et al., 2006, 2009; Proulx et al., 2018; Tse et al., 2006, 2013; Tse & Penney, 2008). Differences in the protocol of our passive oddball task with respect to previous studies might explain differences in the temporal profile of the response. The current occurrence probability of rare (i.e., deviant) stimuli was $p = 8\%$ compared to $p = 20\%$ (Low et al., 2006, 2009; Proulx et al., 2018), which could suggest that in our protocol rare tones were likely to be much more unattended. The duration of our tones was 500 ms, that was much longer than usual stimuli duration in oddball studies, i.e. 70–100 ms (Ruusuvirta et al., 2007; Tse & Penney, 2008; Tse et al., 2006, 2013), and longer than 400 ms used in similar EROS settings (Baniqued et al., 2013; Low et al., 2006, 2009). Moreover, we 1500 Hz instead 500 Hz for the rare tone frequency pip and 60 dB SPL instead of 70 db SPL for the loudness (Low et al., 2006, 2009; Proulx et al., 2018). Hence, our protocol might have triggered a different dynamics or slightly different processes that we observed in our EROS analysis. Filtering parameters are very important for the detection of fast optical signals with a low signal-to-noise ratio (Maclin et al., 2003). In this study EROS was bandpass filtered in the range 0.1–10 Hz, compared to 0–5 Hz (Low et al., 2006, 2009), 0.5–10 Hz (Baniqued et al., 2013), 1–10/12 Hz (Tse & Penney, 2008; Tse et al., 2006, 2013), and 2–20 Hz (Proulx et al., 2018) of the other studies.

The differential EROS response occurring at the same time of the N2/P3 ERP showed an activation in the inferior frontal gyrus at the level of left PMd (BA6) for the rare tones. Both action control and action observation require premotor functions and left PMd participates to mapping external action parameters onto the appropriate motor repertoire (Moisa et al., 2012; Stadler et al., 2012). In addition to the premotor functions, our finding supports the hypothesis that the activation of the left PMd may reflect encoding of the semantic features of actions (i.e., cognitive aspects of the sensorimotor sequences associated with the detection of deviant stimuli) (Press et al., 2012). Around at the same time, a pattern of activation opposite to this one for PMd was observed for EROS in the superior frontal gyrus at the level of BA8, near the border of BA46 in the DLPFC. This area was slightly activated by frequent tones, but it was strongly deactivated by rare tones compared to baseline activity. This signal was not observed by Low et al. (2006), but in their study rare tones were less unattended (20% of the total number of stimuli vs. 8% in our protocol). BA46 is mostly related with the executive control of language production (Ardila et al., 2016) and we suggest that the source of the observed signal was rather BA8. This area of right DLPFC is involved in pitch and memory processing of the auditory stimulus (Kumar et al., 2015; Schaal et al., 2017). Hence, our results might suggest that in the passive oddball task this part of BA8 would be more active when a retrieval attempt of the frequent tone succeeded than when it failed.

We observed an optical signal in the left VLPFC (BA44, Broca's area) occurring with N2 ERP component, in agreement with previous studies (Linden et al., 1999; Medvedev et al., 2010; Tse et al., 2006). The activation in BA44 was strong after rare tones and occurred about at the same time of a lesser activated area in the left postcentral gyrus (BA43) after frequent tones. The anterior ventral stream that brings information about the stimuli's characteristics (i.e., processing an object "what" information) projects to VLPFC (Ahveninen et al., 2006; Plakke & Romanski, 2016). Broca's area (BA44 in the left VLPFC) is involved in semantic tasks, in the motor aspect of speech, and in music perception (Bezgin et al., 2014; Flinker et al., 2015; Levitin & Tirovolas, 2009). The activation of BA43 and surrounding areas in STG was reported for abstract auditory representations and mental imagery of speech (Chiang et al., 2013; Tian et al., 2016). The differential spatial pattern of response observed in our results, between BA44 and BA43, might suggest that the oddball task could engage inhibitory processes triggered by deviant stimuli, as suggested in the literature in association with theta band oscillations (Harper et al., 2014; Jonides et al., 1998; Proulx et al., 2018). We did not analyze here these oscillations, but this is certainly an interesting analysis to be developed in our extended experiment and future studies.

Previous studies have shown ERP negative waves at a latency between 300 and 500 ms post-stimulus elicited in target detection and oddball tasks (Codispoti et al., 2006; Kiehl et al., 2006; Low et al., 2006; Stevens et al., 2005), which was observed in our results as a large N500 (N400-like) wave. Our ERP analysis showed that N500 was almost exclusively elicited by rare tones and its amplitude was much larger for Fz, in agreement with the frontal and right hemisphere topographical distribution reported in those previous studies. The N400-like component has been usually reported with a spatial distribution over centro-parietal or centro-posterior sites in lexical decision tasks and in relation to predictability of stimuli and in the inferior frontal regions, if the effect reflected integration difficulty (Kutas & Hillyard, 1984; Kutas & Federmeier, 2000; Lau et al., 2008; Rossi et al., 2013). Our EROS analysis showed an activation at the level of DLPFC, more specifically in the right hemisphere for two close regions across the Brodmann areas BA9 and BA46. Neuroimaging analysis by fMRI reported that the DLPFC corresponding to the areas BA9/BA46 in the right middle frontal gyrus was involved in maintaining integrated information (Collette et al., 2005; Prabhakaran et al., 2000), associated with the acquisition of abstract rules (Monte-Ordoño & Toro, 2017; Sun et al., 2012) and accompanying conscious experience of abstract auditory percepts (Brancucci et al., 2016).

5 Conclusion

The data of the current study demonstrate that cognitive neural dynamics or pre-frontal cortical activity during a passive auditory oddball task can be studied by a non-invasive fast optical imaging technique (EROS) with co-localized EEG measurements. We identified significant co-occurrences of EROS and ERP responses to rare tones. By combining high spatial and temporal resolution we observed that left and right pre-frontal structures were differentially affected. The left dorsal premotor cortex and Broca's area in the left VLPFC were activated by rare tones during the mismatch negativity and N2 ERP components, whereas frequent tones activated a small area in the right superior frontal gyrus involved in memory processing of the auditory stimulus. Moreover, our results showed a significant N500 (N400-like) wave associated with the activity of DLPFC after rare tones, likely related with the maintenance of integrated information.

Acknowledgements We acknowledge the support by the Swiss National Science Foundation, grant no. POLAP1_178329 for MEJ and grant no. IZSEZ0_183401 for RK.

References

Ahveninen, J., Jääskeläinen, I. P., Raij, T., Bonmassar, G., Devore, S., Hämäläinen, M., et al. (2006). Task-modulated "what" and "where" pathways in human auditory cortex. *Proc Natl Acad Sci U S A*, *103*(39), 14608–13.

Alexander, J. E., Polich, J., Bloom, F. E., Bauer, L. O., Kuperman, S., Rohrbaugh, J., et al. (1994). P300 from an auditory oddball task: inter-laboratory consistency. *Int J Psychophysiol*, *17*(1), 35–46.

Apelbaum, J., Silva, E. E., Frick, O., & Segundo, J. P. (1960). Specificity and biasing of arousal reaction habituation. *Electroencephalogr Clin Neurophysiol*, *12*, 829–840.

Ardila, A., Bernal, B., & Rosselli, M. (2016). How Localized are Language Brain Areas? A Review of Brodmann Areas Involvement in Oral Language. *Arch Clin Neuropsychol*, *31*(1), 112–22.

Baniqued, P. L., Low, K. A., Fabiani, M., & Gratton, G. (2013). Frontoparietal traffic signals: a fast optical imaging study of preparatory dynamics in response mode switching. *J Cogn Neurosci*, *25*(6), 887–902.

Bezgin, G., Rybacki, K., van Opstal, A. J., Bakker, R., Shen, K., Vakorin, V. A., et al. (2014). Auditory-prefrontal axonal connectivity in the macaque cortex: quantitative assessment of processing streams. *Brain Lang*, *135*, 73–84.

Blumstein, D. T. (2016). Habituation and sensitization: new thoughts about old ideas. *Anim Behav*, *120*, 255–262.

Brancucci, A., Lugli, V., Perrucci, M. G., Del Gratta, C., & Tommasi, L. (2016). A frontal but not parietal neural correlate of auditory consciousness. *Brain Struct Funct*, *221*(1), 463–72.

Chance, B., Zhuang, Z., UnAh, C., Alter, C., & Lipton, L. (1993). Cognition-activated low-frequency modulation of light absorption in human brain. *Proc Natl Acad Sci U S A*, *90*(8), 3770–3774.

Chiang, T.-C., Liang, K.-C., Chen, J.-H., Hsieh, C.-H., & Huang, Y.-A. (2013). Brain deactivation in the outperformance in bimodal tasks: an FMRI study. *PLoS One*, *8*(10), e77408.

Codispoti, M., Ferrari, V., Junghöfer, M., & Schupp, H. T. (2006). The categorization of natural scenes: brain attention networks revealed by dense sensor ERPs. *Neuroimage*, *32*(2), 583–91.

Collette, F., Olivier, L., Van der Linden, M., Laureys, S., Delfiore, G., Luxen, A., et al. (2005). Involvement of both prefrontal and inferior parietal cortex in dual-task performance. *Brain Res Cogn Brain Res*, *24*(2), 237–51.

Crottaz-Herbette, S., & Menon, V. (2006). Where and when the anterior cingulate cortex modulates attentional response: combined fMRI and ERP evidence. *J Cogn Neurosci*, *18*(5), 766–80.

Delorme, A., & Makeig, S. (2004). EEGLAB: an open source toolbox for analysis of single-trial EEG dynamics including independent component analysis. *J Neurosci Methods*, *134*(1), 9–21.

Delpy, D. T., & Cope, M. (1997). Quantification in tissue near-infrared spectroscopy. *Philos Trans R Soc Lond B Biol Sci*, *352*(1354), 649–659.

Eriksson, J. L., & Villa, A. E. P. (2005). Event-related potentials in an auditory oddball situation in the rat. *BioSystems*, *79*(1–3), 207–212.

Esposito, F., Mulert, C., & Goebel, R. (2009). Combined distributed source and single-trial EEG-fMRI modeling: application to effortful decision making processes. *Neuroimage*, *47*(1), 112–21.

Fabiani, M., & Friedman, D. (1995). Changes in brain activity patterns in aging: the novelty oddball. *Psychophysiology*, *32*(6), 579–94.

Flinker, A., Korzeniewska, A., Shestyuk, A. Y., Franaszczuk, P. J., Dronkers, N. F., Knight, R. T., et al. (2015). Redefining the role of Broca's area in speech. *Proc Natl Acad Sci U S A*, *112*(9), 2871–5.

Gaillard, A. W. (1976). Effects of warning-signal modality on the contingent negative variation (CNV). *Biol Psychol*, *4*(2), 139–54.

Goodin, D. S., Squires, K. C., Henderson, B. H., & Starr, A. (1978). An early event-related cortical potential. *Psychophysiology*, *15*(4), 360–365.

Gratton, E., Fantini, S., Franceschini, M. A., Gratton, G., & Fabiani, M. (1997). Measurements of scattering and absorption changes in muscle and brain. *Philos Trans R Soc Lond B Biol Sci*, *352*(1354), 727–35.

Gratton, G. (2000). "Opt-cont" and "Opt-3D": A software suite for the analysis and 3D reconstruction of the event-related optical signal (EROS). *Psychophysiology*, *37*, S44.

Gratton, G., Brumback, C. R., Gordon, B. A., Pearson, M. A., Low, K. A., & Fabiani, M. (2006). Effects of measurement method, wavelength, and source-detector distance on the fast optical signal. *NeuroImage*, *32*(4), 1576–1590.

Gratton, G., Cooper, P., Fabiani, M., Carter, C. S., & Karayanidis, F. (2018). Dynamics of cognitive control: Theoretical bases, paradigms, and a view for the future. *Psychophysiology*, *55*(3), e13016.

Gratton, G., & Corballis, P. M. (1995). Removing the heart from the brain: compensation for the pulse artifact in the photon migration signal. *Psychophysiology*, *32*(3), 292–299.

Gratton, G., Corballis, P. M., Cho, E., Fabiani, M., & Hood, D. C. (1995). Shades of gray matter: noninvasive optical images of human brain responses during visual stimulation. *Psychophysiology*, *32*(5), 505–509.

Gratton, G., & Fabiani, M. (1998). Dynamic brain imaging: Event-related optical signal (EROS) measures of the time course and localization of cognitive-related activity. *Psychon Bull Rev*, *5*(4), 535–563.

Gratton, G., & Fabiani, M. (2001). Shedding light on brain function: the event-related optical signal. *Trends Cogn Sci*, *5*(8), 357–363.

Gratton, G., & Fabiani, M. (2010). Fast optical imaging of human brain function. *Front Hum Neurosci*, *4*, e00052.

Harper, J., Malone, S. M., & Bernat, E. M. (2014). Theta and delta band activity explain N2 and P3 ERP component activity in a go/no-go task. *Clin Neurophysiol*, *125*(1), 124–132.

Horovitz, S. G., Skudlarski, P., & Gore, J. C. (2002). Correlations and dissociations between BOLD signal and P300 amplitude in an auditory oddball task: a parametric approach to combining fMRI and ERP. *Magn Reson Imaging*, *20*(4), 319–25.

Jausovec, N., & Jausovec, K. (2009). Do women see things differently than men do? *Neuroimage*, *45*(1), 198–207.

Jeong, E., Ryu, H., Jo, G., & Kim, J. (2018). Cognitive Load Changes during Music Listening and its Implication in Earcon Design in Public Environments: An fNIRS Study. *Int J Environ Res Public Health*, *15*(10), e2075.

Jonides, J., Smith, E. E., Marshuetz, C., Koeppe, R. A., & Reuter-Lorenz, P. A. (1998). Inhibition in verbal working memory revealed by brain activation. *Proc Natl Acad Sci U S A*, *95*(14), 8410–3.

Kennan, R. P., Horovitz, S. G., Maki, A., Yamashita, Y., Koizumi, H., & Gore, J. C. (2002). Simultaneous recording of event-related auditory oddball response using transcranial near infrared optical topography and surface EEG. *Neuroimage*, *16*(3), 587–592.

Kiehl, K. A., Bates, A. T., Laurens, K. R., Hare, R. D., & Liddle, P. F. (2006). Brain potentials implicate temporal lobe abnormalities in criminal psychopaths. *J Abnorm Psychol*, *115*(3), 443–53.

Kubota, M., Inouchi, M., Dan, I., Tsuzuki, D., Ishikawa, A., & Scovel, T. (2008). Fast (100–175 ms) components elicited bilaterally by language production as measured by three-wavelength optical imaging. *Brain Res*, *1226*, 124–33.

Kumar, U., Guleria, A., & Khetrapal, C. L. (2015). Neuro-cognitive aspects of "OM" sound/syllable perception: A functional neuroimaging study. *Cogn Emot*, *29*(3), 432–41.

Kutas, M., & Federmeier, K. D. (2000). Electrophysiology reveals semantic memory use in language comprehension. *Trends Cogn Sci*, *4*(12), 463–470.

Kutas, M., & Hillyard, S. A. (1984). Brain potentials during reading reflect word expectancy and semantic association. *Nature*, *307*(5947), 161–163.

Lacadie, C. M., Fulbright, R. K., Rajeevan, N., Constable, R. T., & Papademetris, X. (2008). More accurate Talairach coordinates for neuroimaging using non-linear registration. *Neuroimage*, *42*(2), 717–25.

Lau, E. F., Phillips, C., & Poeppel, D. (2008). A cortical network for semantics: (de)constructing the N400. *Nat Rev Neurosci*, *9*(12), 920–33.

Lee, J., & Kim, S. J. (2010). Spectrum measurement of fast optical signal of neural activity in brain tissue and its theoretical origin. *Neuroimage*, *51*(2), 713–22.

Levitin, D. J., & Tirovolas, A. K. (2009). Current Advances in the Cognitive Neuroscience of Music. *Ann N Y Acad Sci*, *1156*(1), 211–231.

Linden, D. E., Prvulovic, D., Formisano, E., Völlinger, M., Zanella, F. E., Goebel, R., et al. (1999). The functional neuroanatomy of target detection: an fMRI study of visual and auditory oddball tasks. *Cereb Cortex*, *9*(8), 815–23.

Liu, X., Iwanaga, K., & Koda, S. (2011). Circulatory and central nervous system responses to different types of mental stress. *Ind Health*, *49*(3), 265–73.

Low, K. A., Leaver, E., Kramer, A. F., Fabiani, M., & Gratton, G. (2006). Fast optical imaging of frontal cortex during active and passive oddball tasks. *Psychophysiology*, *43*(2), 127–36.

Low, K. A., Leaver, E. E., Kramer, A. F., Fabiani, M., & Gratton, G. (2009). Share or compete? Load-dependent recruitment of prefrontal cortex during dual-task performance. *Psychophysiology*, *46*(5), 1069–79.

Maclin, E. L., Gratton, G., & Fabiani, M. (2003). Optimum filtering for EROS measurements. *Psychophysiology*, *40*(4), 542–7.

Mangalathu-Arumana, J., Beardsley, S. A., & Liebenthal, E. (2012). Within-subject joint independent component analysis of simultaneous fMRI/ERP in an auditory oddball paradigm. *Neuroimage*, *60*(4), 2247–2257.

McCarthy, G., Luby, M., Gore, J., & Goldman-Rakic, P. (1997). Infrequent events transiently activate human prefrontal and parietal cortex as measured by functional mri. *J Neurophysiol*, *77*(3), 1630–1634.

Medvedev, A. V., Kainerstorfer, J., Borisov, S. V., Barbour, R. L., & VanMeter, J. (2008). Event-related fast optical signal in a rapid object recognition task: improving detection by the independent component analysis. *Brain Res*, *1236*, 145–58.

Medvedev, A. V., Kainerstorfer, J. M., Borisov, S. V., Gandjbakhche, A. H., & Vanmeter, J. (2010). "seeing" electroencephalogram through the skull: imaging prefrontal cortex with fast optical signal. *J Biomed Opt*, *15*(6), 061702.

Menon, V., Ford, J. M., Lim, K. O., Glover, G. H., & Pfefferbaum, A. (1997). Combined event-related fMRI and EEG evidence for temporal-parietal cortex activation during target detection. *Neuroreport*, *8*(14), 3029–3037.

Michalewski, H. J., Prasher, D. K., & Starr, A. (1986). Latency variability and temporal interrelationships of the auditory event-related potentials (N1, P2, N2, and P3) in normal subjects. *Electroencephalogr Clin Neurophysiol*, *65*(1), 59–71.

Moisa, M., Siebner, H. R., Pohmann, R., & Thielscher, A. (2012). Uncovering a context-specific connectional fingerprint of human dorsal premotor cortex. *J Neurosci*, *32*(21), 7244–52.

Molnár, M. (1994). On the origin of the P3 event-related potential component. *Int J Psychophysiol*, *17*(2), 129–44.

Monte-Ordoño, J., & Toro, J. M. (2017). Different ERP profiles for learning rules over consonants and vowels. *Neuropsychologia*, *97*, 104–111.

Näätänen, R. (1990). The role of attention in auditory information processing as revealed by event-related potentials and other brain measures of cognitive function. *Behav Brain Sci*, *13*, 201–288.

Näätänen, R., & Picton, T. (1987). The N1 wave of the human electric and magnetic response to sound: a review and an analysis of the component structure. *Psychophysiology*, *24*(4), 375–425.

Nunez, P. (1995). *Neocortical Dynamics and Human EEG Rhythms*. Oxford University Press, New York, NY., xii, 708 pages.

Okada, E., Firbank, M., Schweiger, M., Arridge, S. R., Cope, M., & Delpy, D. T. (1997). Theoretical and experimental investigation of near-infrared light propagation in a model of the adult head. *Appl Opt*, *36*(1), 21–31.

Opitz, B., Mecklinger, A., Von Cramon, D. Y., & Kruggel, F. (1999). Combining electrophysiological and hemodynamic measures of the auditory oddball. *Psychophysiology*, *36*(1), 142–7.

Plakke, B., & Romanski, L. M. (2016). Neural circuits in auditory and audiovisual memory. *Brain Res*, *1640*, 278–88.

Polich, J. (2007). Updating P300: an integrative theory of P3a and P3b. *Clin Neurophysiol*, *118*(10), 2128–2148.

Prabhakaran, V., Narayanan, K., Zhao, Z., & Gabrieli, J. D. (2000). Integration of diverse information in working memory within the frontal lobe. *Nat Neurosci*, *3*(1), 85–90.

Press, C., Weiskopf, N., & Kilner, J. M. (2012). Dissociable roles of human inferior frontal gyrus during action execution and observation. *Neuroimage*, *60*(3), 1671–7.

Proulx, N., Samadani, A.-A., & Chau, T. (2018). Quantifying fast optical signal and event-related potential relationships during a visual oddball task. *Neuroimage*, *178*, 119–128.

Rinne, T., Gratton, G., Fabiani, M., Cowan, N., Maclin, E., Stinard, A., et al. (1999). Scalp-recorded optical signals make sound processing in the auditory cortex visible? *Neuroimage*, *10*(5), 620–4.

Rossi, S., Hartmüller, T., Vignotto, M., & Obrig, H. (2013). Electrophysiological evidence for modulation of lexical processing after repetitive exposure to foreign phonotactic rules. *Brain Lang*, *127*(3), 404–14.

Ruusuvirta, T., Huotilainen, M., & Näätänen, R. (2007). Preperceptual human number sense for sequential sounds, as revealed by mismatch negativity brain response? *Cereb Cortex*, *17*(12), 2777–9.

Ruusuvirta, T., Korhonen, T., Arikoski, J., & Kivirikko, K. (1996). ERPs to pitch changes: a result of reduced responses to standard tones in rabbits. *Neuroreport*, *7*(2), 413–416.

Schaal, N. K., Kretschmer, M., Keitel, A., Krause, V., Pfeifer, J., & Pollok, B. (2017). The Significance of the Right Dorsolateral Prefrontal Cortex for Pitch Memory in Non-musicians Depends on Baseline Pitch Memory Abilities. *Front Neurosci*, *11*, e00677.

Scholkmann, F., Kleiser, S., Metz, A. J., Zimmermann, R., Mata Pavia, J., Wolf, U., et al. (2014). A review on continuous wave functional near-infrared spectroscopy and imaging instrumentation and methodology. *Neuroimage*, *85*, 6–27.

Squires, N. K., Squires, K. C., & Hillyard, S. A. (1975). Two varieties of long-latency positive waves evoked by unpredictable auditory stimuli in man. *Electroencephalogr Clin Neurophysiol*, *38*(4), 387–401.

Stadler, W., Ott, D. V. M., Springer, A., Schubotz, R. I., Schütz-Bosbach, S., & Prinz, W. (2012). Repetitive TMS suggests a role of the human dorsal premotor cortex in action prediction. *Front Hum Neurosci*, *6*, e00020.

Steinbrink, J., Kempf, F. C. D., Villringer, A., & Obrig, H. (2005). The fast optical signal-robust or elusive when non-invasively measured in the human adult? *Neuroimage*, *26*(4), 996–1008.

Steinbrink, J., Kohl, M., Obrig, H., Curio, G., Syré, F., Thomas, F., et al. (2000). Somatosensory evoked fast optical intensity changes detected non-invasively in the adult human head. *Neurosci Lett*, *291*(2), 105–8.

Stevens, M. C., Calhoun, V. D., & Kiehl, K. A. (2005). Hemispheric differences in hemodynamics elicited by auditory oddball stimuli. *Neuroimage*, *26*(3), 782–792.

Strait, M., & Scheutz, M. (2014). What we can and cannot (yet) do with functional near infrared spectroscopy. *Front Neurosci*, *8*, e00117.

Sun, F., Hoshi-Shiba, R., Abla, D., & Okanoya, K. (2012). Neural correlates of abstract rule learning: an event-related potential study. *Neuropsychologia*, *50*(11), 2617–24.

Syré, F., Obrig, H., Steinbrink, J., Kohl, M., Wenzel, R., & Villringer, A. (2003). Are VEP correlated fast optical signals detectable in the human adult by non-invasive nearinfrared spectroscopy (NIRS)? *Adv Exp Med Biol*, *530*, 421–31.

Talairach, J. and Tournoux, P. (1988). *Co-Planar Stereotaxic Atlas of the Human Brain. 3-Dimensional Proportional System: An Approach to Cerebral Imaging*. Georg Thieme Verlag.

Thompson, R. F. (2009). Habituation: a history. *Neurobiol Learn Mem*, *92*(2), 127–134.

Tian, X., Zarate, J. M., & Poeppel, D. (2016). Mental imagery of speech implicates two mechanisms of perceptual reactivation. *Cortex*, *77*, 1–12.

Torricelli, A., Contini, D., Pifferi, A., Caffini, M., Re, R., Zucchelli, L., et al. (2014). Time domain functional nirs imaging for human brain mapping. *Neuroimage*, *85*, 28–50.

Tse, C.-Y., & Penney, T. B. (2008). On the functional role of temporal and frontal cortex activation in passive detection of auditory deviance. *Neuroimage*, *41*(4), 1462–70.

Tse, C.-Y., Rinne, T., Ng, K. K., & Penney, T. B. (2013). The functional role of the frontal cortex in pre-attentive auditory change detection. *Neuroimage*, *83*, 870–879.

Tse, C.-Y., Tien, K.-R., & Penney, T. B. (2006). Event-related optical imaging reveals the temporal dynamics of right temporal and frontal cortex activation in pre-attentive change detection. *Neuroimage*, *29*(1), 314–20.

Tseng, Y.-L., Lu, C.-F., Wu, S.-M., Shimada, S., Huang, T., & Lu, G.-Y. (2018). A Functional Near-Infrared Spectroscopy Study of State Anxiety and Auditory Working Memory Load. *Front Hum Neurosci*, *12*, e00313.

Verleger, R. (1988). Event-related potentials and cognition: A critique of the context updating hypothesis and an alternative interpretation of P3. *Behav Brain Sci*, *11*(3), 343–356.

Villringer, A., & Chance, B. (1997). Non-invasive optical spectroscopy and imaging of human brain function. *Trends Neurosci*, *20*(10), 435–42.

Walz, J. M., Goldman, R. I., Carapezza, M., Muraskin, J., Brown, T. R., & Sajda, P. (2013). Simultaneous EEG-fMRI reveals temporal evolution of coupling between supramodal cortical attention networks and the brainstem. *J Neurosci*, *33*(49), 19212–22.

Wolf, M., Wolf, U., Choi, J. H., Gupta, R., Safonova, L. P., Paunescu, L. A., et al. (2002). Functional frequency-domain near-infrared spectroscopy detects fast neuronal signal in the motor cortex. *Neuroimage*, *17*(4), 1868–75.

World Medical Association. (2013). World Medical Association Declaration of Helsinki: ethical principles for medical research involving human subjects. *JAMA*, *310*(20), 2191–4.